International Journal of Pure and Applied Physics.
ISSN 0973-1776 Volume 13, Number 3 (2017), pp. 301-316

http://www.ripublication.com

Concentration Quenching Effects in Samarium Doped Zinc Phosphate Glasses for Visible Applications

B. Venkata Rao[1,3], R. Jeevan Kumar[2,3,*], K. Venkata Rao[4]

[1] Loyola Degree College, Pulivendula-516 390, A.P., India.

[2]Department of Physics, Sri Krishnadevaraya University, Anantapur- 517 003, A.P., India.

[3]Department of Physics, JNTU University, Aanantapur-515 002, A.P., India.

[4] S.B.V.R. Degree College, Badvel – 516 227, A.P., India.

Abstract

With interest in the luminescence properties of samarium, six series of phosphate glass composition doped with samarium (0.1, 0.3, 0.5, 1.0, 1.5 and 2.0 mol%) were prepared by melt quenching method, and their luminescence has been investigated. Structural properties are accomplished from XRD (X-Ray Diffractometer) and Raman spectra. Spectroscopic properties are investigated by measuring optical absorption spectra, excitation spectrum, emission spectra and decay profiles. Environment of samarium in phosphate host glass matrix can be accessed by Judd-Ofelt theoretical approach. This theory gives three important parameters such as Ω_2, Ω_4 and Ω_6. In turn these parameters are further used to calculate emission properties certain Sm^{3+} transitions. Luminescence parameters such as stimulated emission cross-sections (σ_p) and branching ratios (β_{exp}) have been studied through photoluminescence spectra. By adjusting the doping concentration in glass system, the quenching and energy transfer effects of samarium were studied. The optimal doping concentration of these phosphate glasses are 0.3 mol% of samarium. The PL spectra for all glasses show four emission bands centred between 564, 601, 643 and 706 nm, owing to the $^4G_{5/2} \rightarrow {}^6H_{5/2}$, $^6H_{7/2}$, $^6H_{9/2}$, and $^6H_{11/2}$ transition of Sm^{3+} ions, respectively. Further, decay time constants are

*Corresponding author email address: rjkskuphy@yahoo.com

estimated from the decay profiles of Sm^{3+} doped different phosphate glasses. An electric dipole–dipole interaction might be the dominant mechanism involved in the energy transfer among between samarium ions, as it was revealed from decay time data. This approach shows significant promise the present prepared zinc phosphate glasses for use in reddish-orange lighting applications.

Keywords: Rare earth doped glasses; Judd-Ofelt theory; Emission properties; Absorption; Decay profiles; Raman spectrum.

1. INTRODUCTION

Various host lattices like glasses, crystals and polycrystalline doped with rare earth ions show efficient emission. Choice of material and their combinations are possible to dope rare earth ions. Glass is flexible and a good host for rare-earth (RE) ions. It exhibit high optical transparency, good rare earth ion solubility, and it can be cast in a variety of shapes or sizes. Luminescent glasses have attracted much attention in the last decades, in particular for optical fibres, laser materials and optical amplifiers [1]. The native luminescence is enhanced by surrounding coordination environment and its composition. We have different ways for getting high emission intensity in any host by, (1) doping with single rare earth (RE) active ion into the suitable single host, (2) co doping with suitable RE ions with different emissions into a single host matrix and then excited simultaneously and, (3) co doping with different active ions in one matrix and controlling the emission intensity through energy-transfer trend [2].

The choice of host materials is also an important task when one deals with improving the efficiency of the luminescence processes. Phosphate glass has high mechanical, good chemical and high thermal stability. Rare earth phosphates are significant due to their bright properties, especially for optical. An extensive curiosity in phosphate glass is confirmed by many publications on luminescence of RE ions in phosphate glasses in recent years. For several applications, the information of the radiative quantum efficiency and lifetime of the optical material are of important parameters. For luminescence point of view, the colour intensity and appropriate doping impurity with different rare-earth ions becomes important aspects [3].

However, drawback of phosphate glass is owing to easy attack towards hydroxyl (OH) groups which dominates non-radiative emission of RE ions than radiative emission. By addition of somewhat fluorine content reduces the OH level in phosphate glasses [4]. The quantum efficiency of active RE ions can be increased by decreasing of multiphonon relaxation rates and inturn increases their emission lifetimes. In addition, phosphate glasses show an enhancement of RE radiative emission properties due to their variety of sites available for the doping ions [5].

The rare-earth ion samarium gained a great technological relevance. For useful applications, the light produce at longer wavelength (red or orange) due to its $^4G_{5/2} \rightarrow {}^6H_J$ (J = 5/2, 7/2, 9/2, 11/2) transitions, is the most suitable sources for solid state lighting and display devices. Their red luminescence was, used in CRT tubes, optical data storage media and plasma displays, and hence got important study [6]. Samarium has been used as local structure probes [7] due to the electric-dipole (ED) character of the $^4G_{5/2} \rightarrow {}^6H_{9/2}$ emissive hypersensitive transition whose intensity increases with increase in environmental asymmetry around samarium ions.

Recently, Ramteke et al. [8] investigated spectroscopic studies of Sm^{3+}/Dy^{3+} co-doped lithium-boro silicate glasses. Zhongli Wu et al. [9] studied optical transition properties, energy transfer mechanism and luminescent thermal stability of Sm^{3+}-doped silicate glasses .Franziska Steude et al. [10] highlighted quantum efficiency and energy transfer processes in rare-earth doped borate glass for solid-state lighting. Herrera et al. [11] prepared B_2O_3–PbO–Bi_2O_3–GeO_2 glass doped with Sm^{3+} and gold nanoparticles.

In this paper describes about the structure, optical and PL properties of samarium in phosphate glasses. The influence of samarium impurity level on the PL properties was investigated. By adjusting the doping concentration in glass system, to study the quenching and energy transfer effects of samarium. Evaluation of the different emission parameters from the luminescence dynamical process and fluorescence lifetime measurements was done.

2. EXPERIMENTAL TECHNIQUES

Different zinc phosphate glasses were prepared by using raw materials (99.9%), ammonium phosphate ($NH_4H_2PO_4$), lithium fluoride (LiF), strontium oxide (SrO), zinc oxide (ZnO) and samarium oxide (Sm_2O_3). The glass compositions details as follows (mol%):

1 Sm01 59.9$NH_4H_2PO_4$-10LiF-10SrO-20ZnO-0.1Sm_2O_3

2 Sm03 59.7$NH_4H_2PO_4$-10LiF-10SrO-20ZnO-0.3Sm_2O_3

3 Sm05 59.5$NH_4H_2PO_4$-10LiF-10SrO-20ZnO-0.5Sm_2O_3

4 Sm10 59.0$NH_4H_2PO_4$-10LiF-10SrO-20ZnO-1.0Sm_2O_3

5 Sm15 58.5$NH_4H_2PO_4$-10LiF-10SrO-20ZnO-1.5Sm_2O_3

6 Sm20 58.0$NH_4H_2PO_4$-10LiF-10SrO-20ZnO-2.0Sm_2O_3

Precise amounts of the starting materials in mol% were weighed out and grinded in an agate mortar. The mixtures were placed in porcelain crucibles and were

then heated in an electric furnace. After heating, the obtained liquid was poured on brass plate and then pressed by another brass plate. The obtained glasses are used for measurements.

Amorphous nature of prepared glasses was verified by SEIFERT X-RAY diffractrometer. Raman spectrum is recorded JOBIN YVUON spectrometer. The optical absorption spectral recording was done on ELICO SL 218 double beam spectrophotometer. The excitation, photoluminescence spectra and decay curves of Sm^{3+} doped glass samples were recorded using FLS-980 fluorescence spectrometer with xenon lamp as excitation source.

3. RESULTS AND DISCUSSION

3.1 XRD analysis

XRD profile of 0.3 mol% of samarium doped phosphate glass is pictured in Fig.1. From this figure, it is apparent that no characteristic diffraction peaks, indicating that the prepared glasses are of amorphous in nature.

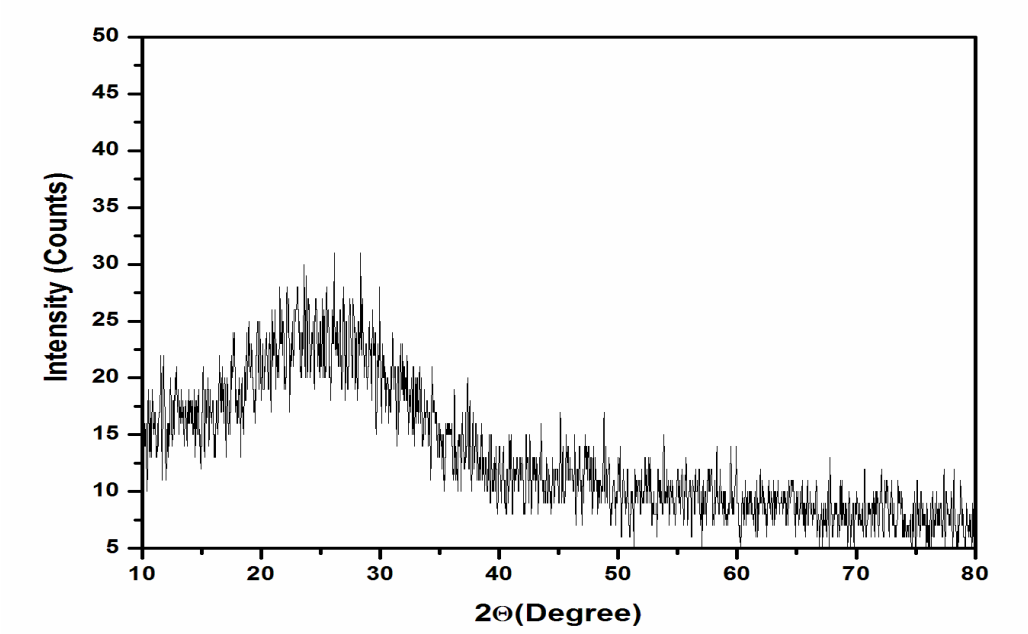

Fig.1. XRD pattern for 0.3 mol% Sm3+ doped zinc phosphate glass matrix

3.2. Raman spectra

Fig.2 shows Raman spectra of 0.3 mol% doped zinc phosphate glass matrix. The low frequency band extended from 300-480 cm^{-1} region is related to the bending motion of phosphate polyhedral PO_4 units with cation like ZnO,SrO etc. as the modifier. The

broad band at 773 cm^{-1} is due to symmetric stretching of (P–O–P) bridging oxygen bonds in $(P_2O_7)^4$ units. [12, 13, 14]. This peak is a convolution of two peaks i.e. one may due to vibrations of the two joined Q^2 units and the second one to those of Q^1 units. Presence of last two bands indicates that due to addition of different modifiers into glass matrix, long range order of network become cut down and formed chain like units. This type of structural units increases glass strength.

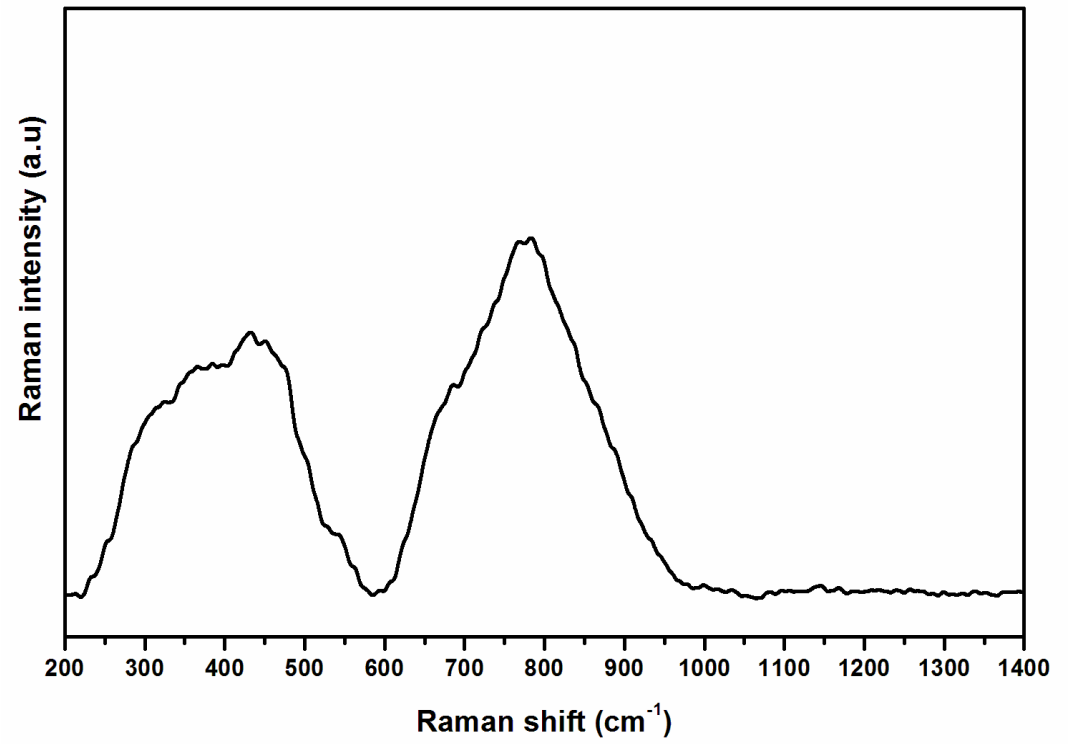

Fig.2 Raman spectrum of 0.3 mol% Sm3+ doped zinc phosphate glass matrix

3.2 Absorption spectra and Judd-Ofelt theory

Absorption spectrum for 0.3mol% of samarium doped zinc phosphate glass is shown in Fig.3a and 3b. From absorption spectrum, optical transitions are investigated. From UV-NIR spectrum, the major absorption bands lies at 404 nm (Sm^{3+}: $^6H_{5/2}\rightarrow{}^2P_{3/2}$) and at 1250 nm ($Sm^{3+}$: $^6H_{5/2}\rightarrow{}^6F_{7/2}$), which are characteristic for Sm^{3+} activated optical glass materials. A weak feature at 17000 cm^{-1} is pertaining to transition in the near NIR (Fig.3b). The absorption bands and their transition assignments from ground state $^6H_{5/2}$ to higher excited states are presented in the spectrum and these transitions labelled according Ref [8, 9, 10]. In the present work, bands are appearing well in the ultraviolet region relatively, even though absorption band of host glass lie in the ultraviolet region and some of the transitions are overlapped with adjust levels.

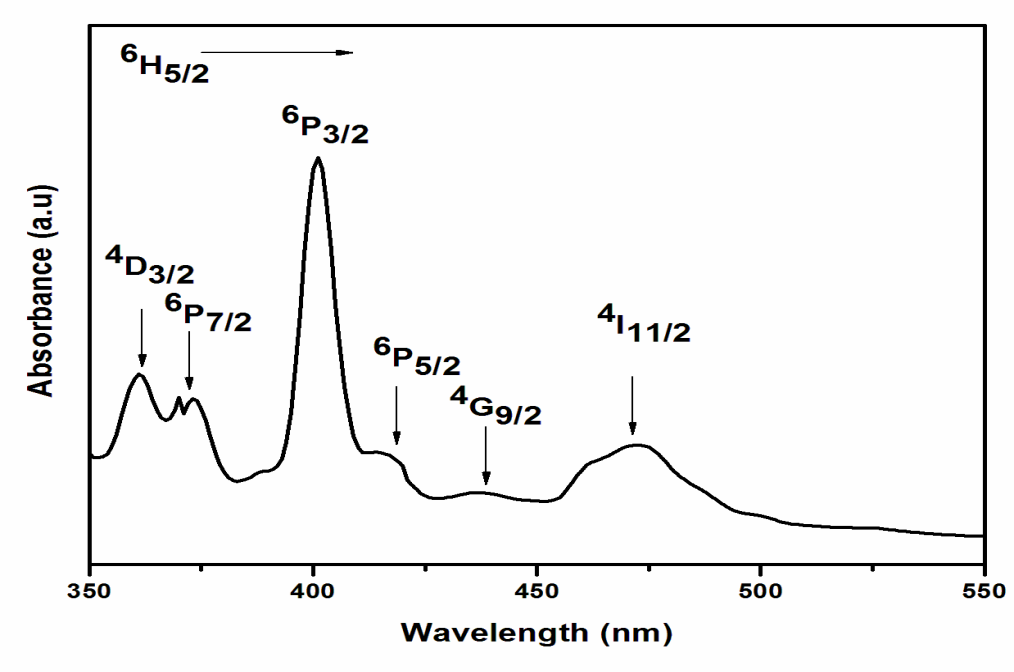

(a)

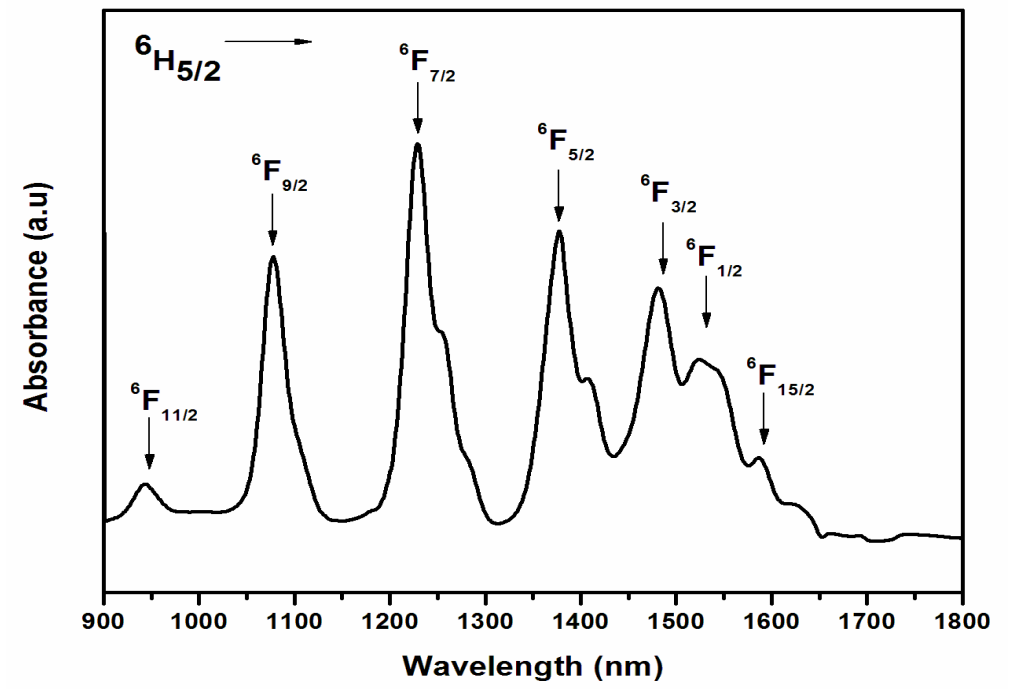

(b)

Fig.3. (a) UV-VIS (b) NIR Absorption spectrum for 0.3 mol% Sm3+ doped zinc phosphate glass matrix

The oscillator strengths or spectral intensity for transitions, (from the absorption spectrum) are considered and are used to evaluate the Judd-Ofelt parameters, using least-squares fitting approach. The calculated (f_{cal}) and experimental (f_{exp}) spectral intensities and their corresponding each transition are tabulated in Table 1. The details of formulas are taken from Ref. [15, 16]. Table 1, depicts the spectral intensities of Sm^{3+} for 0.3 mol% along with root mean square (RMS) deviations. RMS deviation is a measure of difference between spectral intensity values of experimental (from absorption spectra) and calculated (from JO theory) one. From Table 1, it is observed that lower magnitude of RMS deviation indicating that calculation process is reliable. Theory behind the work has been taken from Ref [17].

Table 1

Experimental (f_{exp}) and calculated (f_{cal}) spectral intensities ($x10^{-6}$) and Judd-Ofelt parameters (Ω_λ x 10^{-20} cm^2) of 0.3 mol% of Sm^{3+} doped zinc phosphate glass matrix

Transitions	f_{exp}	f_{cal}
$^4D_{3/2}$	0.14	0.72
$^6P_{7/2}$	1.39	1.31
$^6P_{3/2}$	3.98	4.08
$^6P_{5/2}$	0.36	0.62
$^4G_{9/2}$	0.23	0.06
$^4I_{11/2}$	1.19	1.00
$^6F_{11/2}$	0.30	0.29
$^6F_{9/2}$	2.20	2.30
$^6F_{7/2}$	3.72	3.54
$^6F_{5/2}$	2.38	2.27
$^6F_{3/2}$+$^6F_{1/2}$	1.17	1.14
RMS Deviation	±0.27	
Ω_2	0.51	
Ω_4	3.42	
Ω_6	2.51	

The radiative transitions within the $4f^2$ configuration of Sm^{3+} ion can be analyzed by the Judd-Ofelt theory based on the absorption spectrum of Sm^{3+} ion. Among the three J-O parameters, Ω_2 parameter is due to asymmetric potential of local environment or covalency arises between Sm^{3+} and O^{2-} ligand because of occupancy of samarium ions in different coordination environment. Distortions at position of samarium site may also contribute effectively to covalency or asymmetric environment. The other two parameters *viz.*, Ω_4 and Ω_6 are connected with the bulk properties such as rigidity, viscosity and vibrational levels of the bonding of central samarium ions bound with the surrounding oxygen/fluorine ligand atoms.

Judd-Ofelt intensity parameters Ω_t (t = 2, 4 and 6) are derived to be $0.51x10^{-20}$ cm^2, $3.42x\ 10^{-20}$ and $2.51x10^{-20}$ cm^2 for 0.3 mol% of samarium doped zinc phosphate glass matrix, respectively and are included in Table 1. In the present glass system, JO parameters follow the tendency as $\Omega_4>\Omega_6>\Omega_2$. Ω_2 is higher than the values of $0.42x10^{-20}$ cm^2 in heavy metal borate [11] and $1.23x10^{-20}$ cm^2 in tellurite glass [18]. These magnitudes indicated that the prepared glasses have high covalent bond between samarium and oxygen bond compared with above glass compositions. Ω_2 is lower than the values of $1.23x10^{-20}$ cm^2 in potassium yattrium double phosphates [19] and $3.50x10^{-20}$ cm^2 in alkaline earth borate [20] glasses, showing a weak asymmetrical and covalent environment around 0.3 mol% of Sm^{3+} doped glass matrix. The differences in the distortion around the samarium position lead to variation of covalency and asymmetry in the titled glass matrix. Such decrement or weaker nature, there by decreases degree of disorder in the glass network. Weaker field around Sm^{3+} ions causes to decrease the value of Ω_2 parameter.

3.3. Emission analysis

For the Sm^{3+}-doped Sm03 glass matrix, excitation spectrum is recorded and is shown in Fig. 4. The five peaks are observed in the excitation spectrum represent the transitions of dysprosium ion i.e. $^6H_{5/2}\rightarrow{}^4D_{1/2}+{}^6P_{7/2}$(373 nm), $^6H_{5/2}\rightarrow{}^4F_{7/2}$ (401 nm), $^6H_{5/2}\rightarrow{}^4M_{19/2}$ (417 nm), $^6H_{5/2}\rightarrow{}^4G_{9/2}$ (439 nm) and $^6H_{5/2}\rightarrow{}^4I_{11/2}+{}^4I_{13/2}+{}^4M_{15/2}$ (470 nm). Approximately, 401 nm ($^6H_{5/2}\rightarrow{}^4F_{7/2}$) excitation peak of samarium is selected as the excitation wavelength to measure the luminescence spectra [21].

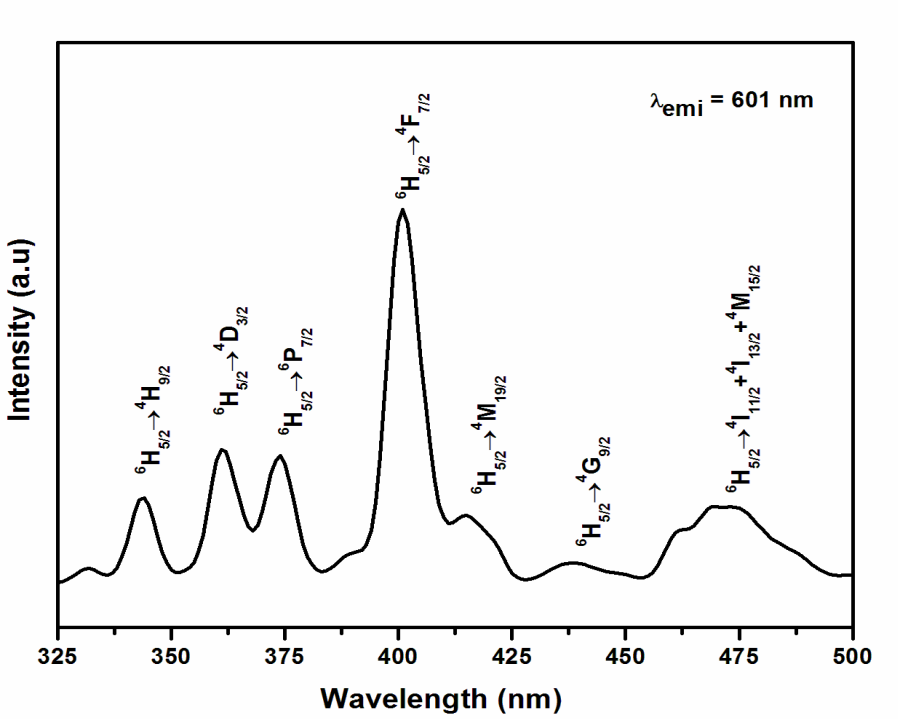

Fig.4 Excitation spectrum of 0.3 mol% Sm^{3+} doped zinc phosphate glass matrix

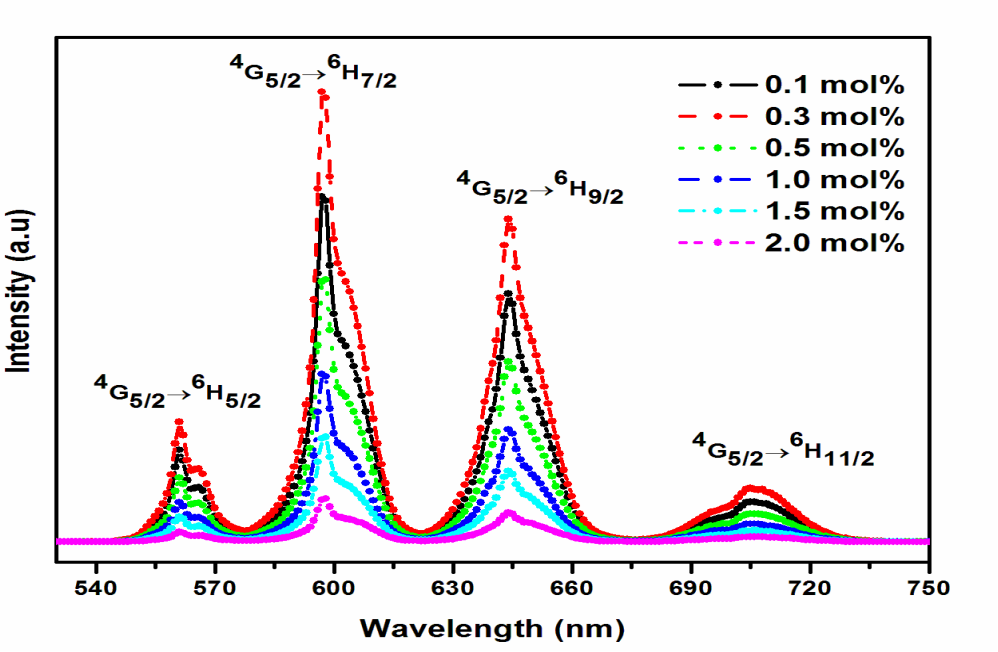

Fig.5 Emission spectra of various concentrations of Sm^{3+} doped zinc phosphate glasses

Samarium emission characteristic peak lines appeared as shown in Fig. 5 and the corresponding characteristic emission peaks of samarium ion are most likely assigned to $^4G_{5/2} \rightarrow {}^6H_{5/2}$ at 564 nm, $^6H_{7/2}$ at 601 nm, $^6H_{9/2}$ at 643 nm and $^6H_{11/2}$ at 706 nm which shows four characteristic Sm^{3+} emission bands. Four of these peaks originate from the Sm^{3+} lowest emitting state $^4G_{5/2}$. It is seen that a very strong visible signal is detected in the reddish-orange (centered at $\lambda \approx 601$ nm) and slightly less powerful signals at 708 nm. In the present work, from emission spectra it is observed that with increase of nominal concentration of samarium, the emission intensity also increases. The higher output luminescence intensity is reached for the content of the glass samarium ions about 0.3 mol%. The bright luminescence observed for the Sm03 glass matrix is reflective of a good optimization between composition-concentration and Sm^{3+} emissive states. While the $^4G_{5/2} \rightarrow {}^6H_{5/2}$ transition is does not appreciably depend on the concentration of samarium doping in Fig. 3. However, the hypersensitive $^4G_{5/2} \rightarrow {}^6H_{9/2}$ transition is magnetic dipole (MD) forbidden and electric-dipole (ED) allowed and its intensity increases as the environmental asymmetry become higher. Higher in the intensity ratio of emissions $^4G_{5/2} \rightarrow {}^6H_{9/2}$ to $^4G_{5/2} \rightarrow {}^6H_{5/2}$ is indicating that the higher in environmental asymmetry and covalency of the luminescent ions.

One can see that during increasing concentration from 0.1 mol% to 0.3 mol%, the emission intensity is enhanced in three fold times and then decreases. The main reason of such decrement should be due to the concentration quenching. Also, at lower concentrations of samarium ions (up to 0.3 mol%) the samarium coordinates with nonbridging oxygens which is responsible for the higher luminescence intensity. At higher concentrations (>0.3 mol%), samarium ions coordinate with bridging oxygens. The interaction between phosphate groups and oxygen groups through samarium ions decreases, i.e. connectivity decreases. Hence, there is a possibility of decreasing fluorescence intensity. The concentration clusters also be a principal for the differences in the behaviour of the luminous. Due to the ion-ion interaction, some transferring processes occurred in samarium doped zinc phosphate glass matrix.

From emission data, luminescence parameters like transition probabilities (A_R), luminescence branching ratios (β_{exp}), effective emission bandwidths ($\Delta\lambda_{eff}$) and stimulated emission cross-sections (σ_e) are calculated for all glasses [3,4] and is presented in Table 2 for the Sm03 glass matrix. The emission transition, $^4G_{5/2} \rightarrow {}^6H_{7/2}$ shows the higher radiative transition rate (A_R: 165 s^{-1}) than other emission transitions. The magnitude of branching ratios characterizes the lasing potential of an emission transition. From Table 2, the $^4G_{5/2} \rightarrow {}^6H_{7/2}$ transition is showing higher branching ratios (49%) which is highly suitable for than other transitions. The predicted β_{exp} are found to be higher for those transitions which are having maximum A_R values. The level having relatively large values of transition probability (A_R), branching ratios (β) and energy gap to next lower level may exhibit good and efficient emission properties and are reported in Table 2.

Table 2

Emission band positions (λ_P, nm), effective bandwidths ($\Delta\lambda_{eff}$, nm), radiative transition probabilities (A_R, s^{-1}), peak stimulated emission cross-sections ($\sigma_{P,}$ $x10^{-22}$ cm^2),experimental branching ratios (β_{exp}) of $^4G_{5/2}$ state for the 0.3 mol% Sm^{3+} doped zinc phosphate glass matrix

Transition	Parameters	Sm03
$^4G_{5/2}\rightarrow{}^6H_{5/2}$	λ_P	564
	$\Delta\lambda_{eff}$	9
	A_R	113
	σ_P	6.65
	β_{exp}	0.07
$^4G_{5/2}\rightarrow{}^6H_{7/2}$	λ_P	601
	$\Delta\lambda_{eff}$	11
	A_R	165
	σ_P	9.84
	β_{exp}	0.46
$^4G_{5/2}\rightarrow{}^6H_{9/2}$	λ_P	643
	$\Delta\lambda_{eff}$	13
	A_R	135
	σ_P	8.69
	β_{exp}	0.38
$^4G_{5/2}\rightarrow{}^6H_{11/2}$	λ_P	706
	$\Delta\lambda_{eff}$	24
	A_R	46
	σ_P	3.01
	β_{exp}	0.09

The stimulated emission cross-section parameter $\sigma(\lambda p)(J,J')$ for transitions between J and J' level and a good luminescent transition should have larger σ_e magnitudes. The materials with large σ_e are utilized to obtain CW laser action [3, 5]. Table 2 gives stimulated emission cross-sections for the observed four emission transitions. Form the table, it is observed that the stimulated emission cross-section is higher for $^4G_{5/2}\rightarrow{}^6H_{7/2}$ transition ($9.84x10^{-22}$ cm^2) among the four transitions and indicating the possible use of this transition for photonic purpose suitable for laser emission.

The ground state $^6H_{5/2}$ of samarium was first excited to higher state $^6P_{3/2}$ when radiation is focused on the samarium glass samples. First, the $^6P_{3/2}$ level is excited and

then the initial population relaxes non-radiatively to the lower $^4G_{5/2}$ emitting level, since the intermediate levels have small vibrational energy differences between the $^6P_{3/2}$ and $^4G_{5/2}$ levels. The ^{4} $G_{5/2}$ level is separated from the next lower lying level ($^6F_{11/2}$) by about 7200 cm^{-1} vibrational energy which is high, so that the multiphonon relaxation (MPR) between these levels is inactive.

As determined from the PL spectrum, the lowest state energy is 22222 cm^{-1}. There are three Sm^{3+} excited states ($^4G_{7/2}$, $^4F_{3/2}$ and $^4G_{5/2}$) that can efficiently absorbs excitation source energy from the lowest state. However, intense emission is only observed from the $^4G_{5/2}$ level. This is owing to the closeness of three states, which causes electrons depopulated from the higher states to the $^4G_{5/2}$ level, from which emission take place. The energy level structure of samarium excited by 401 nm radiation is shown in the Fig.6.

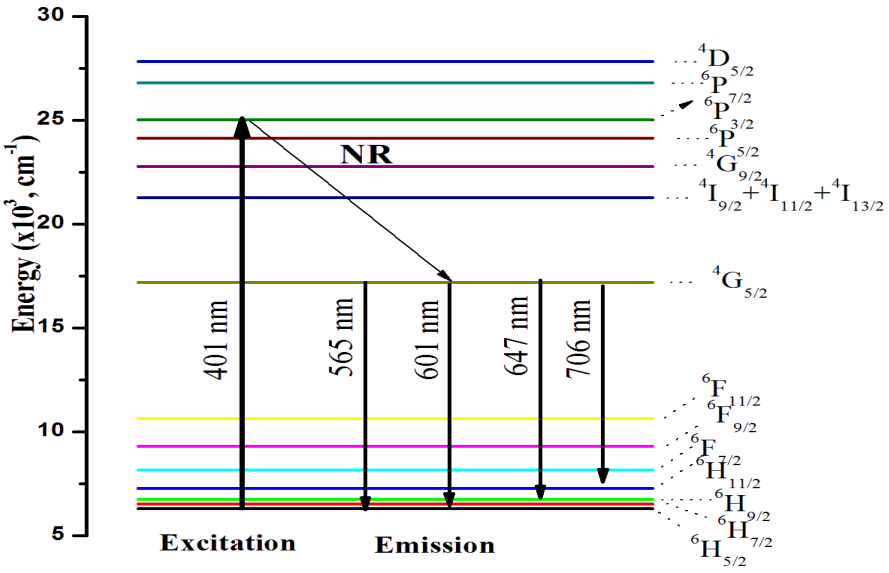

Fig.6 Energy level scheme of Sm^{3+} doped zinc phosphate glass matrix

The energy is lost due to nonradiative processes at higher concentrations. The average Sm–O distance is expected to be relatively smaller in the glass sample containing 0.1 and 0.3 mol% of Sm^{3+} ions concentration and the concentration of higher than this forms probable Sm^{3+} clusters that hinders PL emission intensity.

3.4. Decay analysis

Excited at 404 nm and monitored at 601 nm, the decay profiles of Sm^{3+} doped zinc phosphate glasses are measured. Fig.7 shows the decay curves of zinc phosphate glass

samples with different doping concentrations of samarium ion. From Fig.7, the decay curves resolved with single exponential function for Sm01 amd Sm03 (0.1 and 0.3 mol%) and changed into non-exponential nature for Sm05, Sm10, Sm15 and Sm20 glasses. The emission intensities and decay times showing similar behaviour of concentration quenching. The lifetimes are obtained by e folding times for the studied glasses and presented in Table 3. The decay lifetimes are found to be 1.25, 1.03, 0.90, 0.81, 0.73 and 0.52 ms for 0.1, 0.3, 0.5, 1.0, 1.5 and 2.0 mol% containing zinc phosphate glasses respectively. It is obviously observed that the decay times show the regular decrease with concentration of samarium ions. The lifetimes decrease with increasing the nominal content of samarium ion. The non-exponential character of the decay curves indicate a dipole-dipole type of interaction behaviour in-between two like Sm^{3+} ions due to higher doping level (>0.3 mol%).

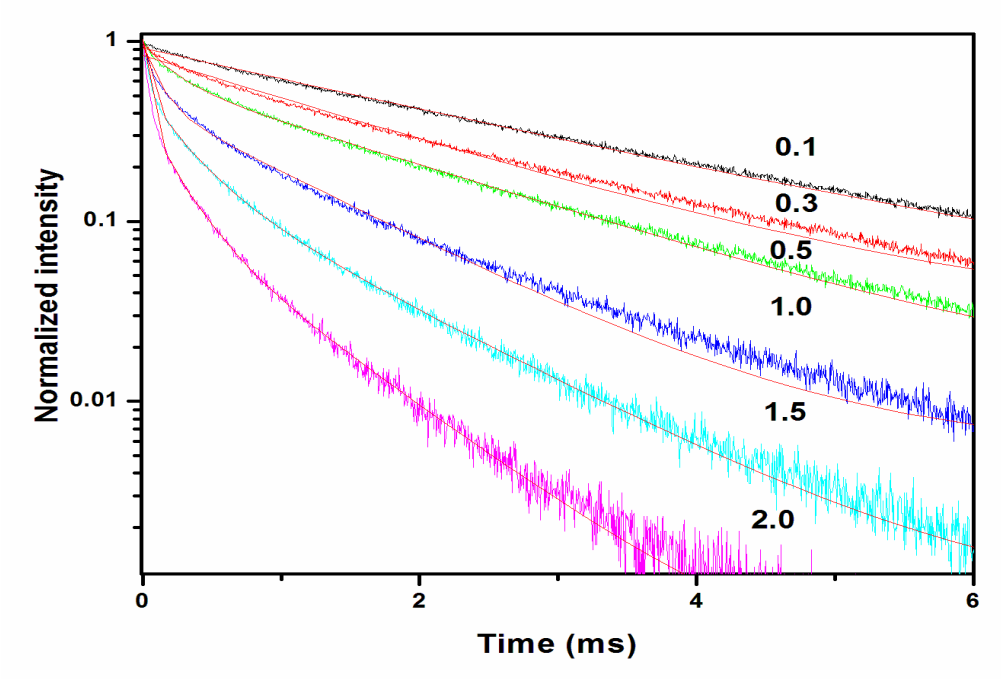

Fig.7 Decay profiles for various concentrations of Sm^{3+} doped of zinc phosphate glasses

At low level of samarium content, the involvement of ion–ion interaction to the decay times is less and the relaxation is dominated by radiative emission transition. The role of the relaxation phenomenon can be approximated through energy gap principle that relates the multiphonon relaxation rate (MPR) and the no of phonons which are needed to cross the energy difference between them. The $^4G_{5/2}$ level possesses purely radiative relaxation process as this level has higher energy gap (~7,000 cm^{-1}) with respect to the next lower lying $^6F_{11/2}$ level and negligible effect of MPR phenomenon.

Any non-exponential character of the fluorescence decay levels accompany by a fast decrease of lifetimes is attributed to the energy transfer (ET) between two similar

samarium atoms. Rare earth ions including Sm^{3+} in amorphous zinc phosphate glass systems form aggregates or clusters in which cross relaxation can give rise to non-radiative de-excitation resulting in short lifetimes. Low intensity and short emission lifetimes exhibited by the glass Sm20 indicates that the possible presence of larger concentration of Sm^{3+} ion clusters that may cause luminescence quenching through ET. In order to investigate the process involved in the ET mechanism, the non-exponential decay curves for the $^4G_{5/2}$ level of Sm^{3+} ions have been analyzed using Inokuti–Hirayama (I-H) model [10]. Best fits of the experimental decays are obtained for S=6 and indicating the ET through cross-relaxation is due to dipole–dipole type of interaction between Sm^{3+} ions.

Acceptor and donor density become more means simultaneously increases enhancement in ET through cross-relaxation (CR) behaviour seems to be appear. The possible CR channels in the Sm^{3+} ion are: ($^4G_{5/2}$ $^6H_{5/2}$)-($^6F_{5/2}$, $^6F_{11/2}$) and ($^4G_{5/2}$, $^6H_{5/2}$)-($^6F_{9/2}$, $^6F_{7/2}$). This CR is due to the ET from the Sm^{3+} ion in an excited $^4G_{5/2}$ state to a nearby Sm^{3+} ion in the ground $^6H_{5/2}$ state (Fig. 6). This transfer leaves the first ion in the intermediate level of $^6F_{5/2}$ at around 7283 nm and the second one in $^6F_{11/2}$ at around 10582 cm^{-1}. The lifetime of the 0.3 mol% doped glass system is longer compared with other reported glass systems. As can be seen from Table 4, the decay of 0.1 mol% and 1.0 mol% displayed short and long lived emissions, of samarium doped phosphate glasses.

CONCLUSIONS

In the present investigation, the luminescence properties of samarium have been investigated. Further, structural properties are also measured like XRD (X-Ray Diffractometer) and Raman spectrum. It is confirmed that the prepared glasses are amorphous character though XRD profiles. From Raman spectra, vibrational bands were identified. Spectroscopic properties are investigated by measuring optical absorption spectra, excitation spectrum, emission spectra and decay profiles. Environment of samarium in zinc phosphate host glass matrix can be accessed by Judd-Ofelt theoretical approach. In turn these parameters are further used to estimate emission properties through photoluminescence spectra. Ω_2 value indicates the change in the asymmetric nature of Sm^{3+} in the zinc phosphate glass host which is also clearly indicated by the asymmetry ratio. From emission spectra, in zinc phosphate glasses showed a characteristic emission wavelength with a maximum at 601 nm. The emission intensity of Sm^{3+} doped different zinc phosphate glasses around 601 nm increased greatly at first and then decreased. Initially, the number of stimulated electrons increased with increase in samarium concentration, the emission intensity of the emission peak located at 601 nm increased greatly at first. Emission intensity reach to the maximum at the Sm^{3+} concentration x=0.3 mol%, further the emission

intensities decreases owing to concentration quenching process. The optimal concentration of samarium is at 0.3m mol% in the prepared zinc phosphate glasses. By adjusting the doping concentration in glass system, the quenching and ET effects of samarium were studied. The double exponential profile can be attributed to the different environments experienced by samarium ions within the glass matrix. These results indicate that energy is lost due to cross relaxations. The obtained results in the present case indicate that bright reddish-orange emission achieved at 0.3 mol% samarium ion which has high luminescence intensity, high branching ratios, high transition probability and high emission cross-sections under suitable excitation wavelength.

REFERENCES

[1] F. Steude, S. Loos, Bernd Ahrens, S. Schweizer, J. Lumin. 170 (2016) 770–777.
[2] Alberto JoséFernandez-Carrion, Manuel Ocaña, Jorge García-Sevillano, Eugenio Cantelar, and Ana Isabel Becerro, J. Phys. Chem. C 118 (2014)18035−18043.
[3] Franziska Steudel, Sebastian Loos, Bernd Ahrens, Stefan Schweize , J. Lumin. 170 (2016) 770–777.
[4] F. Huang, X. Liu, L. Hu, D. Chen, Scientific Reports, 4 (2014) 1-9.
[5] R. Morea, A. Miguel, T.T. Fernandez, B. Maté, F.J. Ferrer, C. Maffiotte, J. Fernandez , R. Balda , J. Gonzalo, J. Lumin. 170 (2016) 778–784.
[6] Xiang-lei Wang, Zhi-qiang Liu, Marion A. Stevens-Kalceff, Hans Riesen, Inorg. Chem. 53 (2014) 8839−8841.
[7] J. Liao, Liangbin Liu, Hangying You, Haiping Huang, Weixiong You, Optik 123 (2012) 901– 905.
[8] D.D. Ramteke , Vijay Kumar, H.C. Swart, J. Non-Cryst. Solids 438 (2016) 49–58.
[9] Z.i Wu, B. Chen, , X. Li, J. Zhang, J. Sun[a], H. Zhong, H. Zheng, L. Tong, H. Xia, J. Alloys Compds. 663, (2016) 545–551.
[10] K. Linganna, Ch. Basavapoornima, C.K. Jayasankar, Optics Commun. 344 (2015) 100–105
[11] A. Herrera, S. Buchner, R.V. Camerini, C. Jacinto, N.M. Balzaretti, Opt. Mater. 52 (2016) 230–236.
[12] Pemberton J. E., Latifzadeh L., Fletcher J. P. and Risbud S. H., Chem. Mater., 3 (1991) 195-200.
[13] Ilieva D., Jivov B., Bogacev G., Petkov C., Penkov I, Dimitriev Y., J. Non-Cryst. Solids, 238 (2001) 195-202.
[14] P. Stoch, W. Szczerba, W. Bodnar, M. Ciecinska, Agata Stochd and Eberhard Burkel, Phys. Chem. Chem. Phys., 2014, 16, 19917—19927.
[15] B.R. Judd, Phys. Rev. 127 (1962) 750.

[16] G.S. Ofelt, J. Chem. Phys. 37 (1962) 511.
[17] S. Selvi, K. Marimuthu, G. Muralidharan, J. Luminescence 159 (2015) 207–218.
[18] A. Kumar, D.K. Rai, S.B. Rai, Spectrochimica Acta Part A 59 (2003) 917–925.
[19] M. Sobczyk, D. Szymański, M. Guzik, J. Legendziewicz, J. Lumin. 169 (2016) 794–798.
[20] L. F. Shen, B. J. Chen, E. Y. B. Pun, H. Lin, J. Lumine. 160 (2015) 138-144.
[21] D. Rajesh, A. Balakrishna, Y.C. Ratnakaram, Opt. Mater. 35 (2012) 108–116.